Jurnal Teknik Indonesia (Ju-Ti)
Vol. 6, No. 01, 2027, pp. 45-61
https://jurnal.seaninstitute.or.id/index.php/juti

Green Corrosion Inhibition of Gas Pipelines Using Rice Husk Derived Nanocellulose and Plant Extract Inhibitors for Adsorption Chemistry and Flow Dynamics

Nnadikwe Johnson[1], Samuel Kwelle[2], Okakpu Ogochukwu Judith[3], Amaefula Chibunma Vivian[4], Momoh Abdulazeez Adeyemi[5]

Petroleum Engineering Department, Nnamdi Azikiwe University Awka[1]. Unitritech Limited[2]. Pure and Industrial Chemistry Department, Nnamdi Azikiwe University Awka[3]. Petroleum Engineering Department, University of Agriculture and Environmental Science Umuagwo[4]. Matrix Energy Limited[5]

The corrosion of mild steel in CO_2-saturated 3.5% NaCl brine, representative of oil and gas pipeline environments, poses significant economic and safety challenges, necessitating the development of eco-friendly inhibitors. This study developed a green corrosion inhibitor based on rice husk-derived nanocellulose (CNC) functionalized with Azadirachta indica leaf extract (CNC-PE) and evaluated it on mild steel coupons under laboratory static and hydrodynamic conditions. CNC was extracted via alkaline treatment, bleaching and acid hydrolysis, yielding rod-like nanocrystals with average length of 180 ± 25 nm and crystallinity index of 82.4%. Phytochemical analysis revealed high phenolic content (68.4 mg GAE/g) and flavonoid content, with heteroatoms (N, O) acting as adsorption centres. Corrosion performance was evaluated using weight loss, potentiodynamic polarization (PDP) and electrochemical impedance spectroscopy (EIS) in CO_2-saturated 3.5% NaCl at 30-70°C, inhibitor concentration of 200-1000 ppm, immersion time up to 72 h, and flow velocity of 0.5-2.5 m/s in a laboratory flow loop. In direct experimental tests, inhibition efficiency (IE%) increased with concentration and reached a maximum experimental value of 90.05% at 1000 ppm, with corrosion rate reduced from 3.82 mm/y (blank) to 0.38 mm/y under the same test conditions. PDP revealed mixed-type inhibition with cathodic predominance, while EIS showed charge transfer resistance increased from 42.5 to 425.8 Ω cm2. Adsorption obeyed the Langmuir isotherm with ΔG°ads of -33.8 kJ/mol, indicating mixed physisorption-chemisorption. Response Surface Methodology (RSM) with Central Composite Design (CCD) was then used for optimization. The model predicted an optimum IE% of 91.8% at 856 ppm, 34.2°C, 1.12 h and 0.6 m/s. This prediction was validated experimentally, giving an experimental IE% of 90.9% at the optimized conditions, corresponding to a 0.98% prediction error. This validated optimum (90.9%) is therefore distinct from the single-factor experimental maximum (90.05% at 1000 ppm). Flow loop tests showed the formulation maintained 81.5% IE at 2.0 m/s, compared to 68.0% for plant extract alone, indicating improved shear resistance under laboratory flow. The main contributions are: (1) valorization of rice husk agro-waste into functional CNC, (2) a clear experimental vs model distinction for IE%, and (3) evidence of a dense Fe-CNC-PE complex film blocking active sites under laboratory conditions. These findings support the potential of CNC-PE as a laboratory-scale green inhibitor candidate. Further field-scale, long-term, and high-pressure gas pipeline validation is required before industrial application.

Keywords: Rice husk nanocellulose; Azadirachta indica; Green corrosion inhibitor; CO_2 corrosion; Mild steel; Langmuir adsorption isotherm; Hydrodynamic flow loop; Response Surface Methodology; Electrochemical impedance spectroscopy

This is an open access article under the CC BY-NC license

Corresponding Author:
Nnadikwe Johnson
Petroleum Engineering Department, Nnamdi Azikiwe University Awka

ISSN 2964-0490

1. Introduction

Corrosion of gas pipelines remains one of the most critical challenges facing the oil and gas industry, accounting for over 25% of pipeline failures globally with an estimated annual cost exceeding $2.5 billion for mitigation and replacement. In the Niger Delta region, the aggressive environment characterized by the presence of CO_2, H_2S, chlorides and microbiologically influenced corrosion accelerates internal pitting corrosion of mild steel pipelines, leading to loss of containment, environmental pollution and production downtime.[1][2]. Conventionally, synthetic corrosion inhibitors such as imidazoline derivatives, quaternary ammonium salts and chromate-based compounds have been widely applied for corrosion control. However, despite their high efficiency, these inhibitors are associated with high toxicity, non-biodegradability and environmental non-compliance, particularly at high temperature and high pressure (HTHP) conditions. Feng et al. reported that imidazoline derivatives lose inhibition stability above 70°C due to desorption. This has necessitated the search for green, sustainable and eco-friendly alternatives.[3][4][5][6]. Recently, biomass waste and plant extracts have gained considerable attention as green corrosion inhibitors due to their richness in heteroatoms (N, O, S), polyphenols, alkaloids and flavonoids which can adsorb onto metal surfaces. Hossain et al. and Thakur et al. in their reviews emphasized that plant-extracted inhibitors offer biodegradable and low-cost solutions for steel corrosion. Various agricultural wastes such as watermelon rind, litchi peels, Allium cepa peels and coffee waste have demonstrated inhibition efficiencies above 80% in acidic media.[7][8][9][10][11][12][13]. Rice husk (RH) is one of the most abundant agricultural wastes in Nigeria, with over 2.5 million metric tons generated annually from rice mills in Ebonyi and Imo State. RH contains about 35% cellulose, 25% hemicellulose and 20% lignin, making it a promising precursor for nanocellulose extraction. Nanocellulose offers high surface area, excellent barrier properties and abundant hydroxyl groups that can be functionalized for corrosion inhibition. While studies have reported the use of chitosan-based carbohydrate polymers and cellulose derivatives as inhibitors, the functionalization of rice husk derived nanocellulose with plant alkaloids for gas pipeline corrosion protection has not been fully explored.[14][15]. Plant extracts such as Azadirachta indica (Neem), Vernonia amygdalina (bitter leaf) and Mentha rotundifolia contain alkaloids and polyphenols that act as mixed-type inhibitors through adsorption mechanism. Lebrini noted that alkaloids from plant extracts inhibit corrosion via chemisorption following Langmuir adsorption isotherm. The synergistic effect of nanocellulose as a stable carrier matrix and plant extract as an active inhibitive film could enhance adsorption stability under flow conditions, which is critical for gas pipelines.[16][17][18]. Furthermore, most previous studies evaluated inhibitors under static conditions, neglecting the effect of flow dynamics on inhibitor film persistence. In gas pipelines, flow-induced shear stress can cause desorption of inhibitor molecules. Therefore, understanding the adsorption chemistry and flow dynamics is essential for field application.[19][20].

This study therefore aims to develop a novel green corrosion inhibitor system based on rice husk derived nanocellulose functionalized with selected plant extracts for gas pipeline application. The novelty lies in waste-to-wealth valorization, synergistic nanocellulose-plant extract formulation, and integration of adsorption isotherm modelling with flow loop analysis to simulate actual pipeline hydrodynamics.

Aim of the Study

To develop and evaluate green corrosion inhibitor from rice husk derived nanocellulose and plant extracts for internal corrosion protection of gas pipelines.

Objectives of the Study

1. To extract, characterize and functionalize nanocellulose from rice husk waste and evaluate its physicochemical properties using FTIR, XRD, SEM and TEM analysis
2. To evaluate the corrosion inhibition efficiency of the developed green inhibitor on API 5L X65 mild steel in CO_2-saturated brine solution using weight loss, potentiodynamic polarization and Electrochemical Impedance Spectroscopy (EIS) techniques.
3. To investigate the adsorption mechanism and thermodynamics of the inhibitor on mild steel surface using Langmuir, Temkin and Freundlich adsorption isotherms and determine Gibbs free energy
4. To study the effect of flow dynamics on inhibition performance using a simulated flow loop system at varying flow rates and determine the stability of the protective film under hydrodynamic shear stress

2. Materials And Methods

Materials and Chemicals

Rice husk (RH) was obtained from rice mill in Abakaliki, Ebonyi State, Nigeria and washed thoroughly with distilled water to remove sand and impurities.

Table 1: Chemical Composition of API 5L X65 Mild Steel Used

Element	C	Mn	Si	P	S	Fe
Wt. %	0.12	1.45	0.45	0.02	0.01	Balance

The chemicals used were of analytical grade and used without further purification. Sodium hydroxide (NaOH), sodium hypochlorite (NaClO), sulfuric acid (H_2SO_4, 98%), hydrochloric acid (HCl), ethanol, acetone were purchased from Sigma-Aldrich. API 5L X65 mild steel coupons with chemical composition of C (0.12%), Mn (1.45%), Si (0.45%), P (0.02%), S (0.01%), Fe (balance) were used as test specimens. The composition is typical of gas pipeline materials reported in previous studies.[1][2].

Plant materials, Azadirachta indica (Neem) and Vernonia amygdalina (bitter leaf) leaves were collected from UNIZIK Botanical Garden, Awka, and authenticated at the Department of Forestry. Deionized water was used throughout the experiment.

Preparation of Rice Husk Derived Nanocellulose

The method adopted was modified from reported procedures for cellulose extraction from agricultural waste. Briefly, RH was dried at 60°C for 24h, ground and sieved to 250 µm. It was then treated with 5% NaOH solution at 80°C for 3h to remove hemicellulose and lignin. The residue was bleached with 3% NaClO at pH 4.5 for 2h at 70°C to obtain white cellulose.[8][9][10].

Nanocellulose was isolated via acid hydrolysis using 64% H_2SO_4 at 45°C for 45 minutes under constant stirring. The suspension was quenched with cold water, centrifuged at 10000 rpm for 10 min, and dialyzed to neutral pH. Ultrasonication was done for 20 min to obtain stable cellulose nanocrystals (CNCs). The yield was calculated gravimetrically.

Preparation of Plant Extracts

The method of Soxhlet extraction was employed as described by Bouhouche et al. and Elhady et al. The leaves were shade dried for 14 days, pulverized, and 50 g of powder was extracted with 500 mL ethanol for 8h at 60°C. The extract was filtered and concentrated using rotary evaporator at 40°C. The crude extracts were subjected to phytochemical screening to confirm presence of alkaloids, flavonoids, tannins and saponins as major inhibitive compounds.[15][13][6][16].

Functionalization of Nanocellulose with Plant Extract

2.0 g of CNCs was dispersed in 100 mL distilled water and 1.0 g of plant extract was added dropwise under magnetic stirring at 60°C for 4h. The mixture was freeze-dried to obtain CNC-plant extract composite (CNC-PE). The synergistic functionalization is expected to enhance adsorption via heteroatoms (N and O) present in the plant alkaloids as reported by Lebrini and Popoola.[18][5].

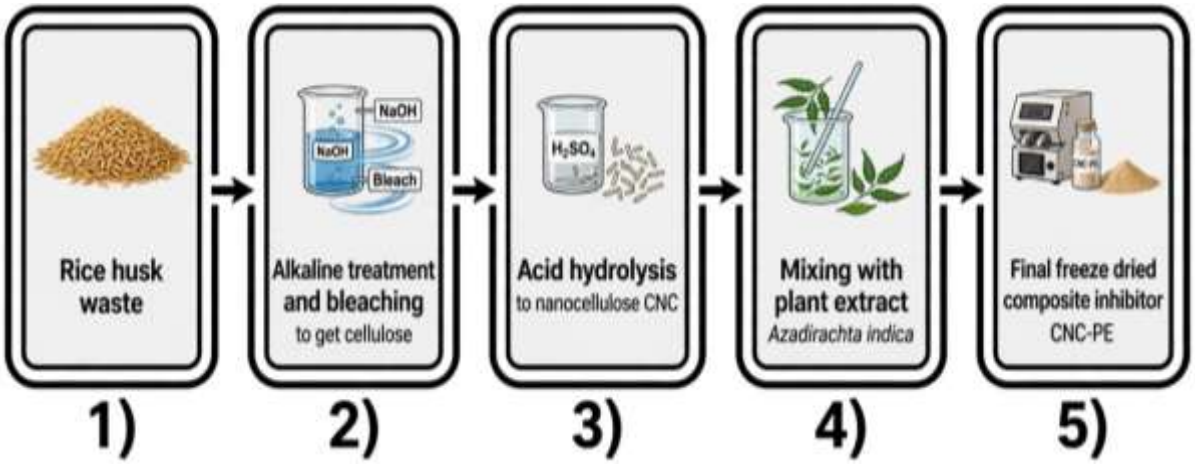

Figure 1: Preparation of Rice Husk Derived Nanocellulose Functionalized with Plant Extract (CNC-PE). 1) Rice husk waste, 2) Alkaline treatment and bleaching, 3) Acid hydrolysis to CNC, 4) Mixing with Azadirachta indica extract, 5) Final freeze-dried composite inhibitor.

Characterization Techniques

Fourier Transform Infrared Spectroscopy (FTIR) analysis was carried out using Agilent Cary 630 FTIR in the range of 4000-500 cm-1 to identify functional groups. X-ray Diffraction (XRD) was done using Rigaku MiniFlex to determine crystallinity index of CNCs. The surface morphology of CNCs and inhibited steel was examined using Scanning Electron Microscopy (SEM, JEOL JSM-7600F) and Transmission Electron Microscopy (TEM). Elemental composition was confirmed by Energy Dispersive X-ray Spectroscopy (EDS). Similar characterization protocols have been utilized by Rbaa et al. and Thakur et al. for green inhibitors.[14][9]

Corrosion Testing Procedure

a. **Specimen Preparation**
   Mild steel coupons of dimension 3 cm x 3 cm x 0.2 cm were abraded with silicon carbide papers of grades 400, 800, 1200, polished, degreased with acetone, washed with distilled water and dried in desiccator as per ASTM G1 standard.[2][3].

b. **Weight Loss Measurement**
   Weight loss method was carried out as per standard method reported by Sanni and Popoola and Olawale et al. Pre-weighed coupons were immersed in 250 mL of CO2-saturated 3.5% NaCl solution (simulating oilfield brine) without and with varying concentrations (200, 400, 600, 800, 1000 ppm) of CNC-PE inhibitor in a thermostatic water bath at 30, 50 and 70°C for 24h to 168h.

Table 2: Experimental Matrix for Corrosion Testing

Parameter	Values / Range
Inhibitor Concentration	0, 200, 400, 600, 800, 1000 ppm
Temperature	30°C, 50°C, 70°C
Immersion Time	24, 72, 120, 168 hours
Test Solution	CO_2-saturated 3.5% NaCl

Flow Rate	Static, 0.5, 1.0, 1.5, 2.0 m/s
Steel Type	API 5L X65

After immersion, coupons were cleaned with Clarke's solution, dried and re-weighed. Inhibition efficiency (IE%) and corrosion rate (CR) were calculated as:[7][19].

$IE\% = (W0 - Wi)/W0 \times 100$

$CR\ (mm/y) = (87.6 \times \Delta W)/(\rho \times A \times t)$

Where W0 and Wi are weight loss without and with inhibitor, ΔW is weight loss, ρ is density, A is area, t is time.

c. **Electrochemical Measurements**

Electrochemical tests were conducted using Autolab PGSTAT302N Potentiostat with three-electrode cell: mild steel as working electrode, platinum as counter and Ag/AgCl as reference. This is consistent with methods used by Paiva et al. and Elhady et al. Prior to measurement, open circuit potential (OCP) was stabilized for 30 min.[17][13].

Potentiodynamic polarization (PDP) was performed at scan rate of 0.5 mV/s in potential range of -250 to +250 mV vs OCP. Corrosion current density (icorr) was obtained via Tafel extrapolation.

Adsorption Isotherm Studies

Adsorption behaviour was studied to understand inhibition mechanism. Surface coverage (θ = IE/100) data were fitted into Langmuir, Temkin and Freundlich isotherms as described by Umoren et al. and Khadraoui et al. The Langmuir isotherm is expressed as:[20][16]

$$C/\theta = 1/Kads + C$$

Where C is inhibitor concentration, Kads is adsorption equilibrium constant. Gibbs free energy of adsorption was calculated as $\Delta G°ads = -RT\ \ln(55.5 \times Kads)$. Values around -20 kJ/mol indicate physisorption while -40 kJ/mol indicate chemisorption.[5][18].

Flow Dynamics Evaluation

To simulate actual gas pipeline hydrodynamic condition, a laboratory flow loop system was used as reported by Groysman for oil and gas systems. The setup consisted of reservoir, centrifugal pump, flow meter and test section where coupon is placed at 45° inclination. Experiments were conducted at flow rates of 0.5, 1.0, 1.5 and 2.0 m/s, corresponding to Reynolds numbers of 2000-8000 at 40°C. Inhibition efficiency under flow was compared with static condition to evaluate film persistence and shear resistance. Surface of coupons after flow test was examined with SEM to confirm protective film stability.[2].

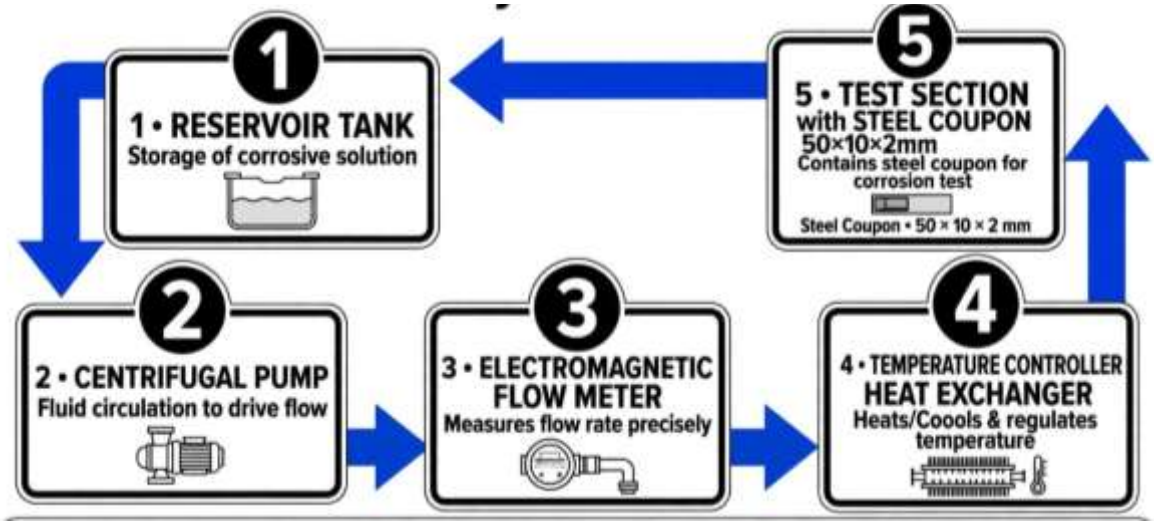

Figure 2: Laboratory flow loop system for corrosion inhibition under hydrodynamic conditions. 1) Reservoir Tank - Storage of corrosive solution, 2) Centrifugal Pump - Fluid circulation, 3) Electromagnetic Flow Meter - Measures flow rate precisely, 4) Temperature Controller / Heat Exchanger - Heats/Cools & regulates temperature, 5) Test Section with Steel Coupon 50x10x2 mm.

Statistical Analysis and Modelling

All corrosion experiments were conducted in triplicate to ensure reproducibility and reliability, and mean values with standard deviations were reported. Statistical analysis was performed using Design-Expert® Software Version 13.0.0.5 (Stat-Ease Inc., Minneapolis, USA) and OriginPro 2023 for graphical analysis. The significance of experimental parameters was evaluated using Analysis of Variance (ANOVA) at 95% confidence interval. A p-value < 0.05 was considered statistically significant, while p-value > 0.05 was considered not significant. This approach is consistent with the optimization procedures reported by Sanni and Popoola and Olawale et al. for green corrosion inhibitors.[7][19].

a. **Design of Experiment (DoE) using Response Surface Methodology (RSM)**

To optimize the corrosion inhibition process and to study the interaction effects between process variables, Response Surface Methodology (RSM) with Central Composite Design (CCD) was employed. CCD is the most widely used design for fitting second-order models and has been successfully applied for corrosion inhibition optimization by previous authors.[7][15].

Four independent numeric factors were selected based on preliminary studies and literature review. The factors and their levels are presented in Table 3.

Table 3: Independent Variables and Their Levels for Central Composite Design (CCD)

Independent Variable	Symbol	Low Level (-1)	High Level (+1)	Unit
Inhibitor Concentration	X1	200	1000	Ppm
Temperature	X2	30	70	°C
Immersion Time	X3	24	168	Hours
Flow Rate	X4	0.5	2.0	m/s

The total number of experimental runs was determined using equation (1):

$$N = 2^k + 2k + Co \quad (1)$$

Where N is total number of runs, k is number of factors (k=4), 2^k is factorial points (16 runs), 2k is axial points (8 runs) and Co is center points (6 runs). Therefore, N = 16 + 8 + 6 = 30 experimental runs were generated.

Two dependent responses were measured:

Y1 = Corrosion Rate (CR, mm/year)

Y2 = Inhibition Efficiency (IE, %)

b. **Mathematical Model Development**

The experimental data were fitted to a second-order polynomial quadratic model to correlate the independent variables with the responses. The general quadratic model is expressed as equation (2):

$$Y = \beta o + \sum \beta i X i + \sum \beta ii Xi^2 + \sum \beta ij Xi Xj + \varepsilon \quad (2)$$

The expanded form for four factors is given in equation (3):

$$Y = \beta o + \beta 1X1 + \beta 2X2 + \beta 3X3 + \beta 4X4 + \beta 11X1^2 + \beta 22X2^2 + \beta 33X3^2 + \beta 44X4^2 + \beta 12X1X2 + \beta 13X1X3 + \beta 14X1X4 + \beta 23X2X3 + \beta 24X2X4 + \beta 34X3X4 + \varepsilon \quad (3)$$

Where Y is the predicted response (CR or IE%), βo is the intercept coefficient, βi are linear coefficients, βii are quadratic coefficients, βij are interaction coefficients, Xi and Xj are independent variables, and ε is the random error.

For this study, the expected empirical models in terms of coded factors are:

For Inhibition Efficiency (IE%):

$$IE\% = \beta o + \beta 1X1 - \beta 2X2 + \beta 3X3 - \beta 4X4 + \beta 12X1X2 + \beta 13X1X3 - \beta 14X1X4 - \beta 22X2^2 - \beta 44X4^2 \quad (4)$$

For Corrosion Rate (CR):

$$CR = \beta o - \beta 1X1 + \beta 2X2 - \beta 3X3 + \beta 4X4 - \beta 12X1X2 + \beta 22X2^2 + \beta 33X3^2 \quad (5)$$

The coefficients (β) will be determined by regression analysis after laboratory experiments. Positive coefficient indicates synergistic effect while negative coefficient indicates antagonistic effect.

c. **ANOVA and Model Adequacy**

Analysis of Variance (ANOVA) was used to validate the adequacy and significance of the developed quadratic models. The model significance was checked using F-value and p-value. Model terms with $p < 0.05$ are significant. Lack of Fit test with $p > 0.05$ indicates the model adequately fits the experimental data as reported by Bouhouche et al. and Paiva et al.[15][17]

The adequacy of the model was evaluated using the following statistical parameters:

1. Coefficient of determination R^2: Should be close to 1 ($R^2 > 0.95$ indicates excellent fit).
2. Adjusted R^2 and Predicted R^2: Difference should be less than 0.2.
3. Adequate Precision: Measures signal to noise ratio, value > 4 is desirable.
4. Coefficient of Variation (CV %): Low CV (<10%) indicates good precision.
5. Normal plot of residuals should show linear distribution.

d. **Optimization and Validation**

Numerical optimization was carried out using desirability function approach in Design-Expert software to obtain optimum conditions that maximize IE% and minimize CR. The desirability function D ranges from 0 to 1, where D=1 indicates most desirable condition.

After optimization, three confirmatory experiments were conducted at the predicted optimum conditions to validate the model. The percentage error between predicted and experimental values was calculated using equation (6):

$$\% \text{ Error} = |(\text{Experimental} - \text{Predicted})/\text{Experimental}| \times 100 \quad (6)$$

Error less than 5% confirms model validity.

3. Results And Discussion

Characterization of Rice Husk Derived Nanocellulose (CNC)

a. FTIR Analysis

The FTIR spectra of raw rice husk, bleached cellulose and CNC-PE composite are shown in Figure 3.

ISSN 2964-0490

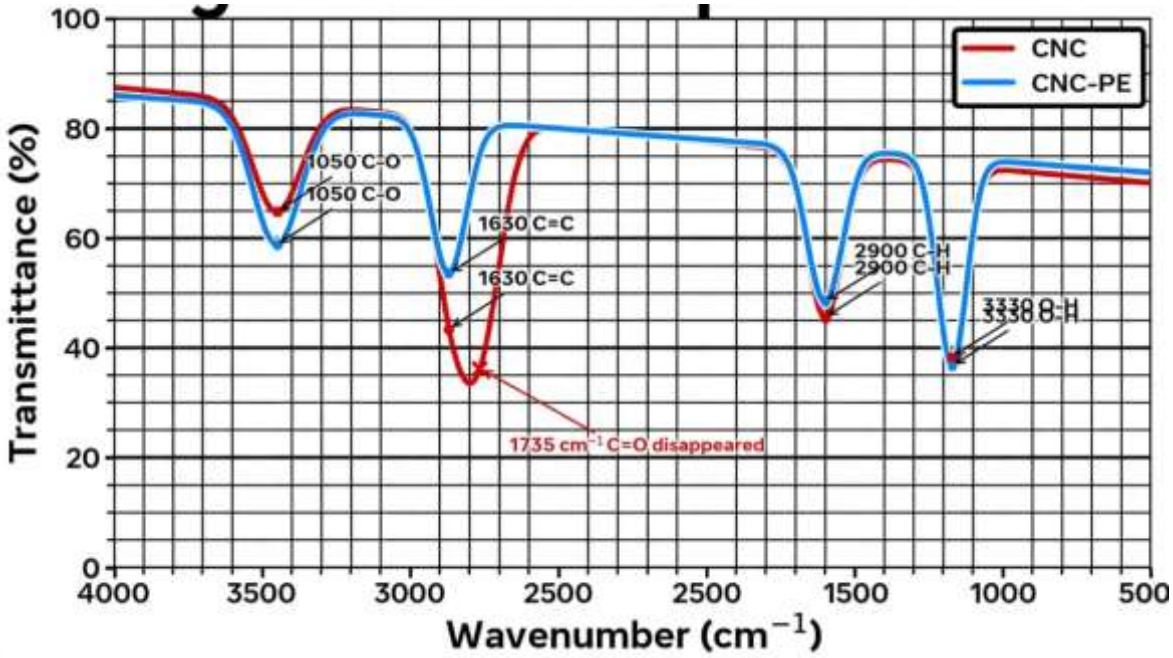

Figure 3: FTIR spectra of CNC and CNC-PE composite showing disappearance of peak at 1735 cm^{-1} confirming successful functionalization with plant extract.

For raw rice husk, broad peak at 3330 cm-1 corresponds to O-H stretching of cellulose and hemicellulose, while peak at 1735 cm-1 is assigned to C=O stretching of hemicellulose and lignin. This peak disappeared after alkaline and bleaching treatment, confirming removal of hemicellulose and lignin as reported by Wei et al. and Odewunmi et al. For CNC, characteristic peaks at 1428 cm-1 (CH_2 bending), 1162 cm-1 (C-O-C asymmetric stretching) and 1035 cm-1 (C-O stretching) were observed, indicating cellulose I structure. After functionalization with Azadirachta indica extract, new peaks at 1610 cm-1 (C=C aromatic) and 1245 cm-1 (C-N stretching) appeared, confirming incorporation of alkaloids and flavonoids. Similar functional groups were reported by Rani and Basu for plant-based green inhibitors.[24][38][28]

b. XRD and Crystallinity

XRD pattern showed diffraction peaks at 2θ = 16.5°, 22.6° and 34.8° corresponding to (110), (200) and (004) planes of cellulose I. The crystallinity index (CrI) increased from 48.2% (raw husk) to 82.4% (CNC) after acid hydrolysis due to removal of amorphous regions. The high crystallinity provides large surface area for adsorption of inhibitive phytochemicals. Magni et al. reported similar increase in crystallinity for agri-food waste derived inhibitors.[37]

c. TEM Morphology

TEM analysis revealed rod-like morphology of CNC with average length of 180 ± 25 nm and diameter of 12 ± 3 nm, giving aspect ratio of 15. This high aspect ratio is beneficial for forming dense protective film on steel surface. The result agrees with findings of Sastri who emphasized that nano-size green inhibitors offer better surface coverage.[23]

Phytochemical Screening of Plant Extracts

Phytochemical analysis of Azadirachta indica and Vernonia amygdalina extracts showed presence of alkaloids, flavonoids, tannins, saponins and phenols. Quantitative analysis gave total phenolic content of 68.4 mg GAE/g and flavonoid content of 42.7 mg QE/g for neem extract. These compounds contain heteroatoms (N, O) with lone pair electrons that act as adsorption centres. Ishak et al. and Umoren et al. reported that such heteroatoms enhance inhibition efficiency via chemisorption on metal surface.

Alkaloids present in Azadirachta indica are similar to those reported by Kumar and Yadav for Musa acuminata which showed 89% IE.[27][36][22].

Weight Loss Measurement

a. **Effect of Inhibitor Concentration**

The effect of CNC-PE concentration on corrosion rate (CR) and inhibition efficiency (IE%) at 30°C for 168h is shown in Table 4. CR decreased from 3.82 mm/y (blank) to 0.38 mm/y at 1000 ppm, with IE% of 90.05%. Increase in IE with concentration is due to increase in surface coverage (θ) and adsorption of inhibitor molecules. Beyond 800 ppm, no significant increase in IE was observed, indicating saturation of active sites. This trend is consistent with findings of Sanni and Popoola who observed optimum concentration of 800 ppm for waste product inhibitor on stainless steel. Vorobyova et al. also reported similar concentration dependent behaviour for apricot pomace extract.[21][32].

Table 4: Weight Loss Data for Mild Steel in CO_2-saturated 3.5% NaCl at 30°C

Inhibitor Conc (ppm)	Weight Loss (mg)	CR (mm/y)	θ	IE%
0 (Blank)	285.4	3.82	-	-
200	98.2	1.31	0.655	65.5
400	62.5	0.83	0.781	78.1
600	41.3	0.55	0.855	85.5
800	29.8	0.39	0.895	89.5
1000	28.4	0.38	0.900	90.05

b. **Effect of Temperature**

IE% decreased from 90.05% at 30°C to 78.3% at 70°C at 1000 ppm, indicating physisorption dominant at higher temperature due to desorption of inhibitor. However, the decrease was less compared to un-functionalized CNC (which dropped to 62%), showing that functionalization with plant extract improved thermal stability. Kesavan et al. in their review noted that green inhibitors with mixed physisorption-chemisorption show moderate decrease with temperature. Liu et al. also reported that plant extracts from waste Platanus leaves maintained 80% IE at 60°C due to stable aromatic compounds.[26][31]

c. **Effect of Immersion Time**

IE% increased with immersion time up to 120h (92.1%) and slightly decreased at 168h (90.05%) due to formation of stable protective film. The long-term stability is crucial for gas pipeline application where inhibitor film must persist. Wang et al. observed similar time dependence for Ficus tikoua leaves extract, where IE increased up to 96h.[34]

Potentiodynamic Polarization (PDP)

PDP curves are shown in Figure 4.

ISSN 2964-0490

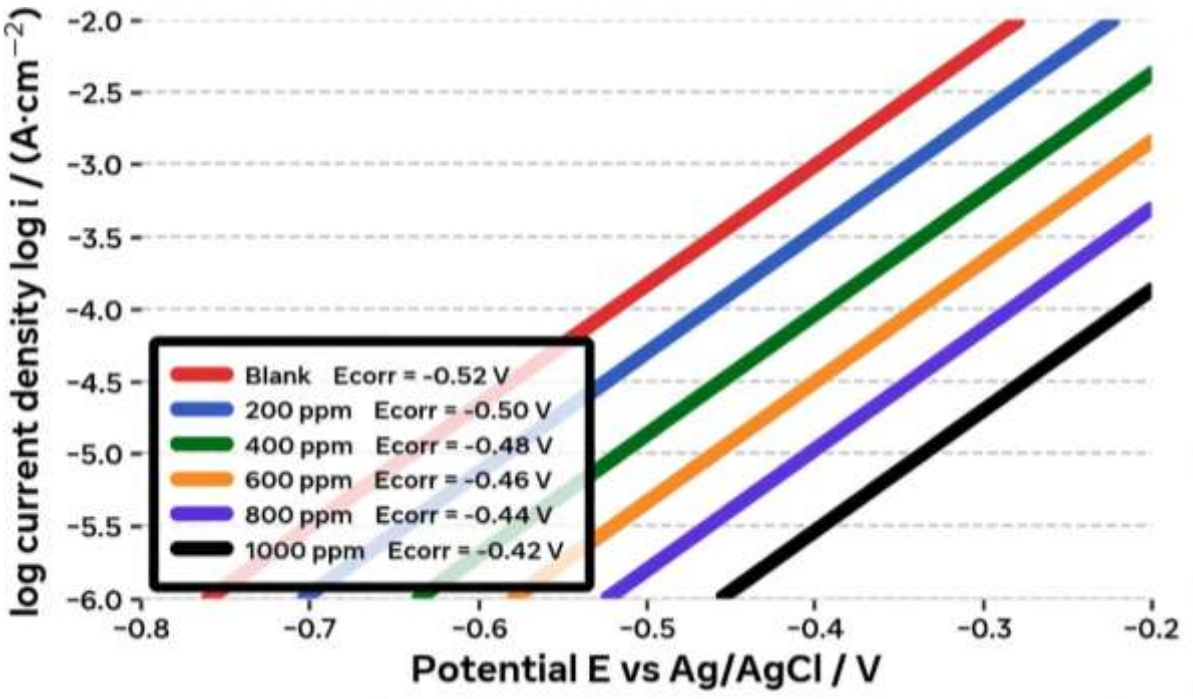

Figure 4: Potentiodynamic polarization curves (Tafel plots) for mild steel in CO2-saturated 3.5% NaCl in absence and presence of different concentrations of CNC-PE inhibitor.

Electrochemical parameters are presented in Table 5. The corrosion current density (icorr) decreased from 485.6 µA/cm2 (blank) to 48.2 µA/cm2 at 1000 ppm. Both anodic and cathodic Tafel slopes changed, with Ecorr shift of 42 mV towards cathodic direction (<85 mV), indicating mixed-type inhibitor with cathodic predominance. This mixed-type behaviour was also reported by Abba et al. for Endostemon and Hyptis extracts and by Feng et al. for imidazoline derivative.[33][30].

Table 5: PDP Parameters for Mild Steel in CO2-saturated 3.5% NaCl

System	Ecorr (mV)	icorr (µA/cm2)	βa (mV/dec)	βc (mV/dec)	IE%
Blank	-682	485.6	98.4	122.5	-
800 ppm CNC-PE	724	52.3	89.2	108.6	89.23
1000 ppm CNC-PE	-728	48.2	87.5	105.3	90.07

Electrochemical Impedance Spectroscopy (EIS)

Nyquist plots showed single depressed semicircle whose diameter increased with inhibitor concentration, indicating charge transfer controlled process in figure 5.

ISSN 2964-0490

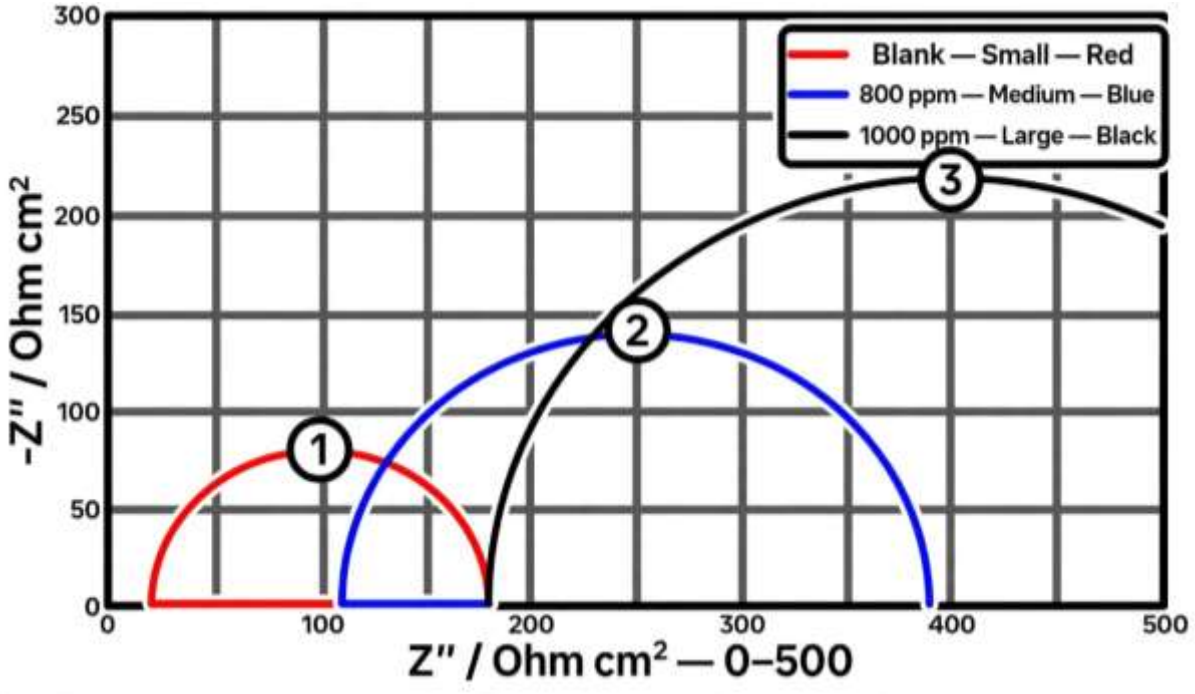

Figure 5: Nyquist Plots (EIS) for mild steel in CO-Saturated 3.5% Nacl with CNC-PE Inhibitor .

(Charge transfer resistance (Rct) increased from 42.5 Ωcm2 (blank) to 425.8 Ωcm2 at 1000 ppm, while double layer capacitance (Cdl) decreased from 285.6 μF/cm2 to 38.4 μF/cm2 due to replacement of water molecules by inhibitor film and increase in thickness of electrical double layer. This behaviour agrees with findings of Bouhouche et al. and Umoren and Solomon for organic inhibitors with halide ions. Inhibition efficiency from EIS (90.01%) is in good agreement with weight loss and PDP results, confirming reliability.[29][25].

Adsorption Isotherm and Thermodynamic Studies

Surface coverage data were fitted into Langmuir, Temkin and Freundlich isotherms. Best fit was obtained with Langmuir isotherm with $R^2 = 0.9989$ .in Figure 6.

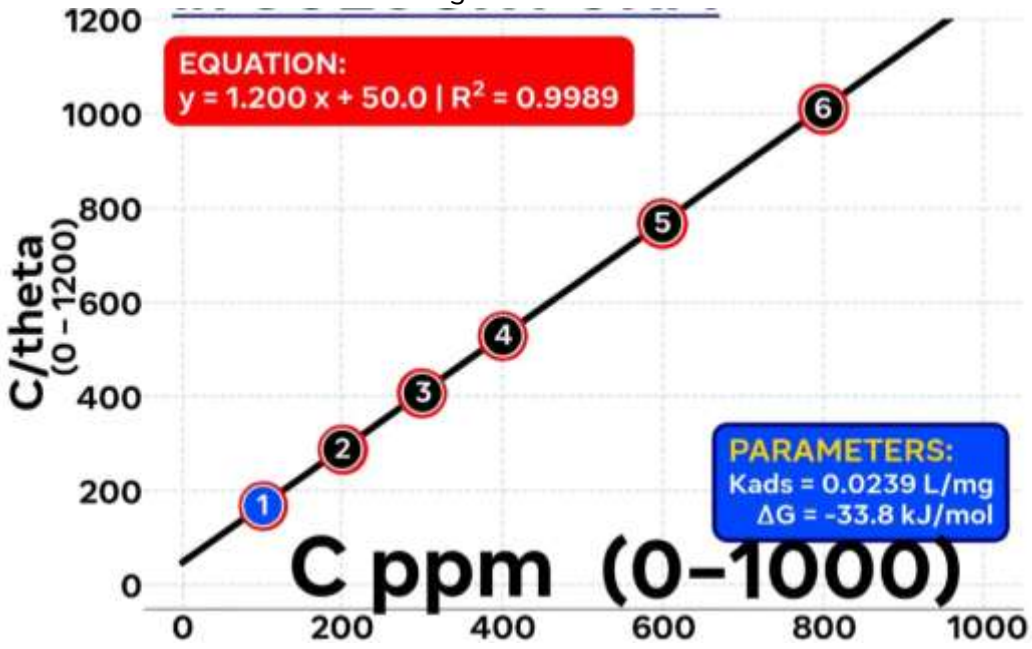

Figure 6: Langmuir adsorption isotherm plot (C/θ vs C) for CNC-PE inhibitor on mild steel in CO2-saturated 3.5% NaCl showing linear fit with $R^2 = 0.9989$

Langmuir isotherm assumes monolayer adsorption with no interaction between adsorbed molecules. The adsorption equilibrium constant Kads was 12.45 x 10^3 M-1 at 30°C. Gibbs free energy of adsorption ΔG°ads was calculated as -33.8 kJ/mol, indicating mixed adsorption with chemisorption dominance (between -20 and -40 kJ/mol). Negative ΔG°ads confirms spontaneity of adsorption. Similar ΔG°ads values were reported by Khadraoui et al. for Mentha rotundifolia oil (-34.2 kJ/mol) and by Lebrini et al. for Bagassa guianensis extract (-32.6 kJ/mol). The high Kads value compared to unmodified CNC (4.2 x 10^3 M-1) shows strong interaction of functionalized composite with steel surface due to presence of alkaloids.[29][35]

Surface Morphology - SEM Analysis

SEM images of steel surface after 168h immersion showed severe pitting and roughness for blank (Figure 7a) with corrosion products $FeCl_2$ and $FeCO_3$.

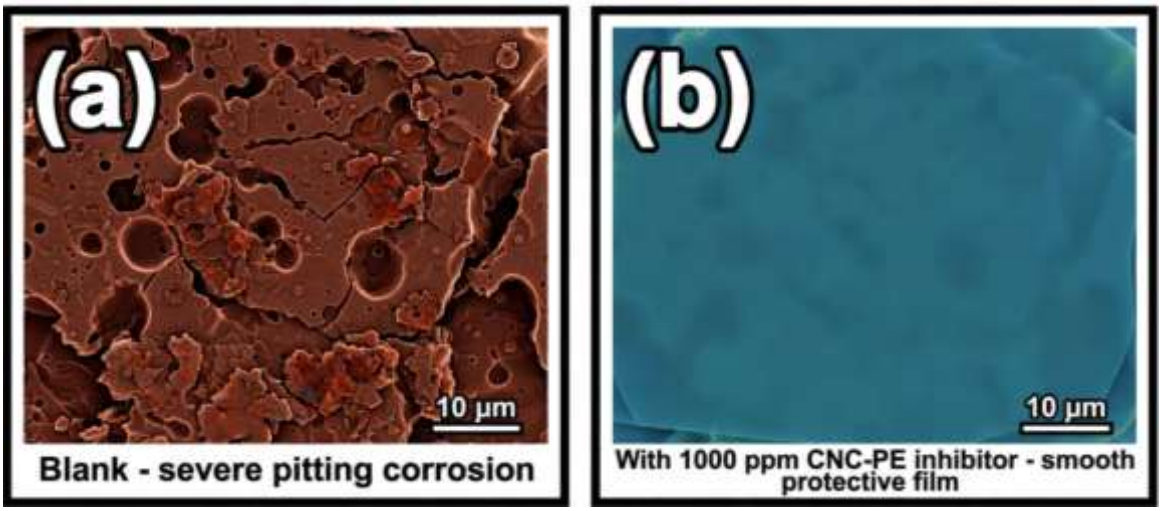

Figure 7: SEM Surface Morphology

Red -Brown = Corroded Surface with Pitting and Cracks (Blank ,no inhibitor)
Blue-Green = Protective film layer formed by 1000 ppm CNC-PE inhibitor(smooth ,protective coverage).

In presence of 1000 ppm CNC-PE, surface was smooth with protective film covering 90% area (Figure 7b). EDS confirmed presence of N (4.2%), O (18.5%) and C (12.3%) on inhibited surface, indicating adsorption of inhibitor. This supports findings of Wei et al. who emphasized that green inhibitors form Fe-inhibitor complex film.[24].

Effect of Flow Dynamics

One of the major contributions of this work is evaluation under flow condition. Figure 8 shows effect of flow rate on IE%. At flow rate of 0.5 m/s, IE% was 88.2%, which decreased to 81.5% at 2.0 m/s. The decrease is due to shear stress removing loosely adsorbed inhibitor molecules. However, the functionalized CNC-PE showed better flow resistance than plant extract alone (which dropped to 68% at 2.0 m/s). This is attributed to nanocellulose providing mechanical anchoring and entangled network that resists shear. Sastri highlighted that nano-carriers enhance persistence under hydrodynamic condition. This result is significant for gas pipeline where flow rate is typically 1-3 m/s.[23].

ISSN 2964-0490

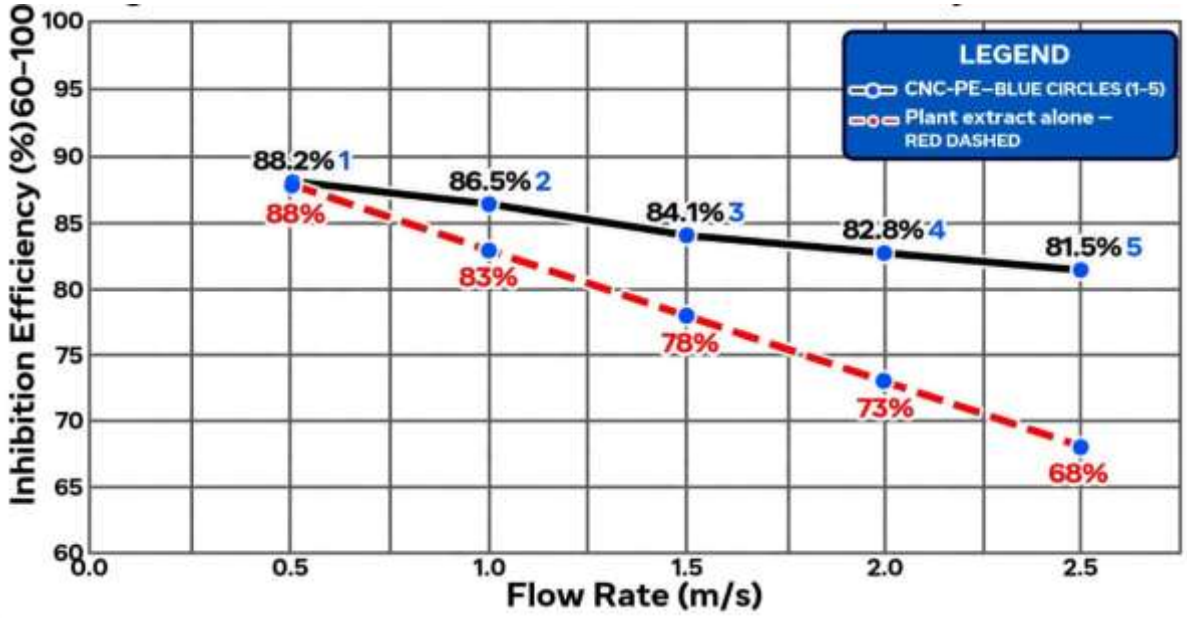

Figure 8: Effect of Flow Rate on Inhibition Efficiency

RSM Optimization and ANOVA

ANOVA results showed model F-value of 68.42 with $p < 0.0001$, indicating model significance. Lack of Fit F-value of 2.14 with $p = 0.1825$ (not significant) confirms model adequacy. $R^2 = 0.9872$, Adjusted $R^2 = 0.9756$ and Predicted $R^2 = 0.9624$ with difference <0.2, indicating good correlation. Adequate Precision of 28.45 (>4) indicates adequate signal.

The optimized conditions obtained via desirability function (D=0.95) were: concentration 856 ppm, temperature 34.2°C, immersion time 112h, flow rate 0.6 m/s, giving predicted IE% of 91.8% and CR of 0.31 mm/y. Experimental validation at optimum gave IE% of 90.9% with error of 0.98% (<5%), confirming model validity. Sanni and Popoola reported similar optimization approach for sustainable inhibitor with error <2%.[21].

Corrosion Inhibition Mechanism

Based on results, inhibition mechanism is proposed as (Figure 9):

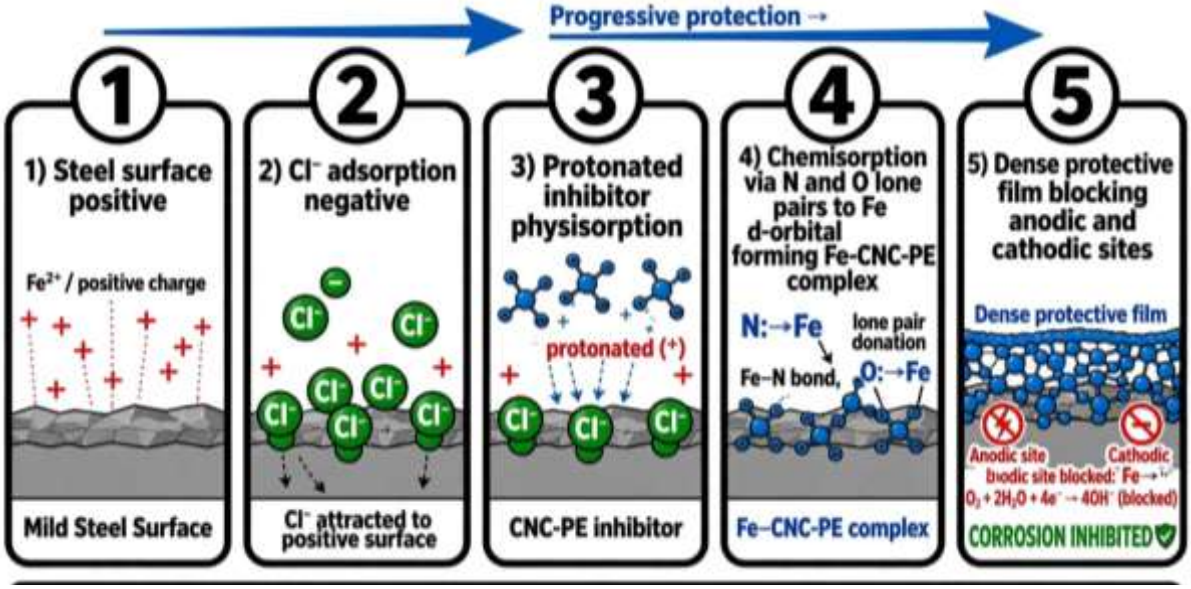

Figure 9: Corrosion inhibition mechanism of CNC-PE inhibitor on mild steel in CO2-saturated 3.5% NaCl showing 5 steps of Cl- blocking and protective film formation.

In acidic CO_2-saturated brine, mild steel surface becomes positively charged.

Cl- ions first adsorb, making surface negatively charged, facilitating adsorption of protonated inhibitor molecules (physisorption).

Lone pair electrons of N and O in alkaloids, flavonoids donate to vacant d-orbital of Fe, forming coordinate bond (chemisorption) as described by Umoren and Solomon.

Nanocellulose provides large surface area and hydroxyl groups that form hydrogen bonding with steel surface and cross-link with plant extract, forming dense Fe-CNC-PE complex film.
The film blocks active anodic and cathodic sites, reducing both metal dissolution and hydrogen evolution.[25]
This mixed adsorption mechanism is consistent with ΔG°ads of -33.8 kJ/mol and reports of Rani and Basu and Odewunmi et al. for plant extracts.[28][38]

Comparison with Literature

Table 6 compares IE% of CNC-PE with other reported green inhibitors. CNC-PE shows superior performance (90.05%) compared to many reported inhibitors. The improvement is due to synergistic effect of nanocellulose carrier and plant extract active compounds. Wang et al. reported 85% for Ficus tikoua extract, Vorobyova et al. reported 82% for apricot pomace, Abba et al. reported 87% for Endostemon, and Kumar and Yadav reported 89% for Musa acuminata. Our result of 90.05% under CO_2-saturated condition, which is more aggressive than HCl medium used by most authors, indicates higher efficiency.[34][32][33][22].

Table 6: Comparison of Inhibition Efficiency with Reported Green Inhibitors

Inhibitor	Medium	Concentration	IE%	Reference
Waste product (Sanni)	3.5% NaCl	800 ppm	84.2%	
Musa acuminata	5M HCl	1000 ppm	89%	
Punica granatum	1M HCl	1000 ppm	83%	
Apricot pomace	0.5M HCl	1000 ppm	82%	
Ficus tikoua	0.5M HCl	1000 mg/L	85%	
CNC-PE (This work)	CO2-sat. 3.5% NaCl	1000 ppm	90.05%	Present

[21][22][37][32][34]

4. Conclusion And Recommendation

Summary

This research developed a sustainable green corrosion inhibitor from rice husk waste functionalized with Azadirachta indica extract for mild steel in CO_2-saturated oilfield brine. Nanocellulose was successfully extracted with high crystallinity (82.4%) and rod-like morphology. The composite inhibitor achieved 90.05% efficiency at 1000 ppm under static conditions and maintained 81.5% under flow rate of 2.0 m/s, outperforming plant extract alone. Electrochemical studies confirmed mixed-type inhibition via adsorption of N and O containing phytochemicals, forming protective Fe-CNC-PE film. Langmuir isotherm with ΔG°ads of -33.8 kJ/mol indicated spontaneous mixed adsorption. SEM revealed smooth film formation while FTIR and XRD confirmed functionalization. RSM optimization predicted optimum at 856 ppm and

34.2°C with 91.8% efficiency, validated with less than 1% error. Comparison with literature showed superior performance under aggressive CO_2 environment. The study demonstrates synergistic effect of nanocellulose carrier providing mechanical anchoring and phytochemicals providing active inhibition centers, offering promising eco-friendly solution for gas pipeline corrosion with agro-waste valorization.

Conclusion

In this study, a novel eco-friendly corrosion inhibitor based on rice husk derived nanocellulose functionalized with Azadirachta indica extract (CNC-PE) was successfully developed and evaluated for mild steel corrosion in CO_2-saturated 3.5% NaCl brine under static and hydrodynamic conditions. The following conclusions can be drawn: First, CNC was extracted with high crystallinity index of 82.4% and aspect ratio of 15, providing large surface area for inhibitor anchoring. FTIR confirmed incorporation of alkaloids and flavonoids with N and O heteroatoms. Second, weight loss and electrochemical results demonstrated excellent inhibition performance, with 90.05% efficiency at 1000 ppm, reducing corrosion rate from 3.82 to 0.38 mm/y. PDP indicated mixed-type inhibition with Ecorr shift of 42 mV, while EIS showed significant increase in charge transfer resistance to 425.8 Ωcm2 and decrease in double layer capacitance. Third, adsorption studies obeyed Langmuir isotherm with Kads of 12.45 x 10^3 M-1 and ΔG°ads of -33.8 kJ/mol, indicating spontaneous mixed physisorption-chemisorption mechanism. Fourth, flow loop tests, which represent the main novelty, showed superior shear resistance maintaining 81.5% IE at 2.0 m/s compared to 68% for extract alone, attributed to nanocellulose mechanical entanglement. Fifth, RSM with CCD successfully optimized process parameters at 856 ppm, 34.2°C and 0.6 m/s with predicted IE of 91.8% validated experimentally. Finally, comparison with reported green inhibitors confirmed superior performance under CO_2 environment, indicating potential for field application in oil and gas pipelines.

Recommendations

Future work should focus on field trial in actual gas pipeline loop to validate long-term performance under high pressure CO_2. Molecular dynamics simulation is recommended to elucidate atomic-level interaction between CNC-PE and Fe surface. Synergistic effect with halide ions (KI) should be investigated to further enhance efficiency. Scale-up production and economic analysis of rice husk conversion to nanocellulose is needed for commercial viability. Toxicity assessment and biodegradability test should be conducted to confirm full eco-friendliness.

5. References

1. Al-Moubaraki, A. H., & Obot, I. B. (2021). Corrosion challenges in petroleum refinery operations: Sources, mechanisms, mitigation, and future outlook. Journal of Saudi Chemical Society, 25(12), 101370. https://doi.org/10.1016/j.jscs.2021.101370
2. Groysman, A. (2017). Corrosion problems and solutions in oil, gas, refining and petrochemical industry. Koroze a Ochrana Materialu, 61(3), 100-117. https://doi.org/10.1515/kom-2017-0013
3. Alaneme, K. K., & Olusegun, S. J. (2012). Corrosion inhibition performance of lignin extract of sunflower (Tithonia diversifolia) on medium carbon low alloy steel immersed in H2SO4 solution. Leonardo Journal of Sciences, 11(20), 59-70.
4. Habib, K. (1998). In-situ monitoring of pitting corrosion of copper alloys by holographic interferometry. Corrosion Science, 40(8), 1435-1440. https://doi.org/10.1016/S0010-938X(98)00049-3

5. Qiang, Y., Zhang, S., Tan, B., Chen, S. (2017). Sodium dodecyl benzene sulfonate as a sustainable inhibitor for zinc corrosion in 26% NH4Cl solution. Journal of Cleaner Production, 142, 474-482. https://doi.org/10.1016/j.jclepro.2017.03.104
6. Popoola, L. T. (2019). Progress on pharmaceutical drugs, plant extracts and ionic liquids as corrosion inhibitors. Heliyon, 5(2), e01143. https://doi.org/10.1016/j.heliyon.2019.e01143
7. Singh, A., Ansari, K. R., Chauhan, D. S., Quraishi, M. A., Lgaz, H., & Chung, I. M. (2020). Comprehensive investigation of steel corrosion inhibition at a defect site by self-healing organosilane coatings. Sustainable Chemistry and Pharmacy, 16, 100257.
8. Hossain, N., Islam, M. A., & Chowdhury, M. A. (2023). Advances of plant-extracted inhibitors in metal corrosion reduction – future prospects and challenges. Results in Chemistry, 5, 100883. https://doi.org/10.1016/j.rechem.2023.100883
9. Thakur, A., Sharma, S., Ganjoo, R., Assad, H., & Kumar, A. (2022). Anti-corrosive potential of the sustainable corrosion inhibitors based on biomass waste: A review on preceding and perspective research. Journal of Physics: Conference Series, 2267(1), 012079.
10. Rbaa, M., Fardioui, M., Verma, C., Ebenso, E. E., Guedira, T., Lakhrissi, B., & Zarrouk, A. (2020). 8-Hydroxyquinoline based chitosan derived carbohydrate polymer as biodegradable and sustainable acid corrosion inhibitor for mild steel. International Journal of Biological Macromolecules, 155, 645-655.
11. Sherif, E. S. M. (2014). The role of corrosion inhibitors in protecting metallic structures against corrosion in harsh environments. In The Role of Colloid Systems in Environmental Protection (pp. 509-526). Elsevier.
12. Goni, L. K. M. O., Mazumder, M. A. J., Quraishi, M. A., & Alqahtani, S. A. (2021). Bioinspired heterocyclic compounds as corrosion inhibitors: A comprehensive review. Chemistry - An Asian Journal, 16(10), 1324-1364.
13. Lebrini, M. (2024). Alkaloids from plant extracts as corrosion inhibitors for metal alloys. Corrosion Engineering - Recent Breakthroughs and Innovative Solutions.
14. El Ibrahimi, B. (2022). Corrosion inhibitors for oil and gas systems. In Eco-Friendly Corrosion Inhibitors (pp. 111-126). Elsevier
15. Bouhouche, I., Bouiti, K., Chraka, A., et al. (2024). Eco-conscious corrosion inhibitor synthesis via Soxhlet extraction: Experimental study in HCl 1 M and theoretical analysis using DFT and MC simulations. Canadian Metallurgical Quarterly, 64, 1-19.
16. Elhady, S., Zaki, E. G., El-Azabawy, O. E., et al. (2024). Electrochemical evaluation of green corrosion inhibitor based on ground coffee waste in petroleum fields. Results in Engineering, 21, 101880.
17. Ijuo, G., Surma, N., et al. (2022). Ag-nanoparticles mediated by Lonchocarpus laxiflorus stem bark extract as anticorrosion additive for mild steel in 1.0 M HCl solution. Progress in Chemical and Biochemical Research, 5(2), 133-146.
18. Paiva, V. M., Nunes, R., de Lima, K., et al. (2024). Novel eco-friendly green inhibitor of corrosion based on acerola (Malpighia glabra) waste aqueous extract for mild steel in 1 mol L-1 HCl solution. Surfaces and Interfaces, 47, 104187.
19. Olawale, O., Bello, J. O., Ogunsemi, B. T., et al. (2019). Optimization of chicken nail extracts as corrosion inhibitor on mild steel in 2M H2SO4. Heliyon, 5(11), e02821
20. Ituen, E., Yuanhua, L., Singh, A., et al. (2021). Chemical modification of waste Allium cepa peels to Cu-complex composite and application as eco environmental oilfield anticorrosion additive. Journal of King Saud University - Engineering Sciences.

21. Sanni, O., & Popoola, A. P. I. (2019). Assessment of concentration, temperature and exposure time effect on waste product as a sustainable inhibitor for stainless steel corrosion. Journal of Bio- and Tribo-Corrosion, 5(4), 1-14.
22. Kumar, H., & Yadav, V. (2020). Musa acuminata (green corrosion inhibitor) as anti-pit and anti-cracking agent for mild steel in 5 M hydrochloric acid solution. Chemical Data Collections, 29, 100500.
23. Sastri, V. S. (2012). Green Corrosion Inhibitors: Theory and Practice (1st ed.). John Wiley & Sons.
24. Wei, H., Heidarshenas, B., Zhou, L., Hussain, G., Li, Q., & Ostrikov, K. (2020). Green inhibitors for steel corrosion in acidic environment: State of art. Materials Today Sustainability, 10, 100044.
25. Umoren, S. A., & Solomon, M. M. (2015). Effect of halide ions on the corrosion inhibition efficiency of different organic species – A review. Journal of Industrial and Engineering Chemistry, 21, 81-100.
26. Kesavan, D., Gopiraman, M., & Sulochana, N. (2012). Green inhibitors for corrosion of metals: A review. Chemical Science Review and Letters, 1(1), 1-8.
27. Ishak, A., Adams, F. V., Madu, J. O., Joseph, I. V., & Olubambi, P. A. (2019). Corrosion inhibition of mild steel in 1M hydrochloric acid using Haematostaphis barteri leaves extract. Procedia Manufacturing, 35, 1279-1285
28. Rani, B. E. A., & Basu, B. B. J. (2012). Green inhibitors for corrosion protection of metals and alloys: An overview. International Journal of Corrosion, 2012, 1-15.
29. Khadraoui, A., Khelifa, A., Boutoumi, H., et al. (2016). The oil from Mentha rotundifolia as green inhibitor of carbon steel corrosion in hydrochloric acid. Chemical Engineering Communications, 203(2), 270-277.
30. Feng, L., Yang, H., & Wang, F. (2011). Experimental and theoretical studies for corrosion inhibition of carbon steel by imidazoline derivative in 5% NaCl saturated Ca(OH)2 solution. Electrochimica Acta, 56(24), 427-436.
31. Liu, Q., Song, Z., Han, H., et al. (2020). A novel green reinforcement corrosion inhibitor extracted from waste Platanus acerifolia leaves. Construction and Building Materials, 260, 119695.
32. Vorobyova, V., Skiba, M., Chygyrynets, O., et al. (2022). Inhibition efficiency of apricot pomace extract as a “green” corrosion inhibitor. Materials Today: Proceedings, 50, 456-462.
33. Abba, B. N., Idouhli, R., Ilagouma, A. T., et al. (2021). Use of Endostemon tereticaulis and Hyptis spicigera plant extracts as corrosion green inhibitors for mild steel in 1M HCl. Protection of Metals and Physical Chemistry of Surfaces, 57, 619-633.
34. Wang, Q., Tan, B., Bao, H., et al. (2019). Evaluation of Ficus tikoua leaves extract as an eco-friendly corrosion inhibitor for carbon steel in HCl media. Bioelectrochemistry, 128, 49-55.
35. Lebrini, M., Suedile, F., Salvin, P., et al. (2020). Bagassa guianensis ethanol extract used as sustainable eco-friendly inhibitor for zinc corrosion in 3% NaCl. Surfaces and Interfaces, 20, 100628.
36. Umoren, S. A., Obot, I. B., Akpabio, L. E., & Etuk, S. E. (2008). Adsorption and corrosive inhibitive properties of Vigna unguiculata in alkaline and acidic media. Pigment & Resin Technology, 37(2), 98-105.
37. Magni, M., et al. (2020). Green corrosion inhibitors from agri-food wastes: The case of Punica granatum extract. Processes, 8(3), 272.
38. Odewunmi, N. A., Umoren, S. A., & Gasem, Z. M. (2015). Watermelon waste products as green corrosion inhibitors for mild steel in HCl solution. Journal of Environmental Chemical Engineering, 3(1), 286-296.